Acta Cryst. (1984). B40, 329–332

Electron Density Distribution in Ilmenite-Type Crystals. II. Manganese(II) Titanium(IV) Trioxide

BY KUMIKO KIDOH, KIYOAKI TANAKA AND FUMIYUKI MARUMO

The Research Laboratory of Engineering Materials, Tokyo Institute of Technology, Nagatsuta 4259, *Midori-ku, Yokohama* 227, *Japan*

AND HUMIHIKO TAKEI

Research Institute for Iron, Steel and Other Metals, Tohoku University, Sendai 980, *Japan*

(*Received* 11 *November* 1983; *accepted* 25 *January* 1984)

Abstract

The electron density distribution in a crystal of $MnTiO_3$ has been investigated with the single-crystal X-ray diffraction method. A small amount of partial disorder was observed in the cation arrangement of the crystal examined. Deformation densities were observed around the Mn^{2+} ion and these are presumed to be due to anharmonic thermal vibration of the ion. No indication of aspherical distribution was detected on the static $3d$ electron density of Mn^{2+}. The electron cloud around the Ti^{4+} ion is deformed to shield the positive charge of the Mn^{2+} ion as in $CoTiO_3$ crystals. A positive-density region spreads between the nearest Mn^{2+} ions in the deformation density map, which may be an indication of direct interaction between the cations. The antiferromagnetic order observed in the (0001) plane at low temperatures does not contradict the existence of direct interaction. [Crystal data: $R\bar{3}$, $a = 5{\cdot}13948(7)$, $c = 14{\cdot}2829(4)$ Å, $Z = 6$, $D_x = 4{\cdot}601$ g cm^{-3}, μ(Mo $K\alpha$) = $89{\cdot}04$ cm^{-1}.]

Introduction

In the previous paper (Kidoh, Tanaka, Marumo & Takei, 1984) the authors reported the results of an investigation on electron density distributions in a crystal of $CoTiO_3$. An aspherical distribution of d electrons around the Co^{2+} ion and a deformation of the electron cloud around the Ti^{4+} ion were observed for this crystal. Ilmenite-type crystals of the first-series transition-metal elements are antiferromagnetic at low temperatures, each having different magnetic structures. Further, correlation of spin is believed to exist within the (0001) planes even above the Néel temperature (Akimitsu, Ishikawa & Endoh, 1970). Therefore, it is of interest to investigate the electron distributions in these crystals in connection with their magnetic structures. In this paper, results of an X-ray investigation on the electron distribution in a crystal of $MnTiO_3$ are described.

Experimental

A crystal synthesized with an infrared-heating floating-zone furnace (Takei, Hosoya & Kojima, 1982) was used as in the case of $CoTiO_3$. A piece of the crystal was shaped into a sphere 0·148 mm in diameter by the Bond (1951) method. Specimen confirmed to have an ilmenite-type structure from Weissenberg photographs. Rigaku automated four-circle diffractometer (AFC-5). Lattice constants determined from 39 2θ values higher than 88°, Mo $K\alpha_1$ radiation. Intensity data collected in a sextant of reciprocal space lower than 150° in 2θ; in addition, a total of 86 strong reflections were measured in full reciprocal space for anisotropic extinction corrections. All remaining experimental conditions are as in the previous paper (Kidoh *et al.*, 1984). Total of 2453 reflections measured, 1259 independent, 1461 with $|F_o| > 3\sigma(|F_o|)$ used for subsequent calculations. Corrections for Lp factors, absorption and extinction as in the previous paper (Kidoh *et al.*, 1984).

Refinement

Two kinds of least-squares refinements were carried out. One was the usual refinement, and the other was performed subsequently taking anharmonic thermal vibrations into consideration.

The structure refinement was started from the ideal ilmenite structure model. Atomic scattering factors for Mn^{2+} and Ti^{4+} ions and dispersion-correction factors were taken from *International Tables for X-ray Crystallography* (1974). The scattering factor given by Tokonami (1965) was used for the O^{2-} ions. The refinement was carried out with a modified version of the full-matrix least-squares program *LINEX* including the extinction corrections after Becker & Coppens (1974*a*, *b*, 1975). Since partial disorder of the cations was observed in $CoTiO_3$ (Kidoh *et al.*, 1984), the chemical formula (Mn_qTi_r)-$(Ti_uMn_v)O_{q+v+2(r+u)}$ was also assumed for the present crystal, and the population parameters were refined

0108-7681/84/040329-04$01.50

with a normalization of the larger value of $q+r$ and $u+v$ to unity. Least-squares calculations assuming type II anisotropic extinction effects gave significantly smaller R and R_w values (0·0123 and 0·0150) than those with type I (0·0135 and 0·0160). The values 0·92(2), 0·08(3), 0·93(3) and 0·06(2) were obtained for q, r, u and v, respectively, giving the chemical formula $(Mn_{0\cdot92}Ti_{0\cdot08})(Ti_{0\cdot93}Mn_{0\cdot06}\square_{0\cdot01})O_3$.

At this stage, the difference Fourier maps were synthesized by averaging equivalent reflections. It was found that both cations lay in negative regions, and positive peaks were observed around them. In particular, the peak near the Mn^{2+} ion on the threefold axis is fairly high and situated too close (0·29 Å) to the cation to be a deformation density of $3d$ electrons. Therefore, a trial was carried out to explain these positive and negative peaks with the anharmonic thermal vibrations of the cations, following the procedure of Willis (1969). For this purpose, a rectangular coordinate system was defined for each of the metal atoms so that the z axis lies along the c axis and x in the plane defined by z and the metal to the shared oxygen bond which is nearest to the $(01\bar{1}0)$ plane. In Willis's method, anharmonic vibration is described as a motion in a one-particle potential of the following form (Willis, 1969; Tanaka & Marumo, 1984),

$$V(\mathbf{u}) = V_0 + \tfrac{1}{2}\sum_i b_i u_i^2 + \sum_i \sum_j c_{ijj} u_i u_j^2 + c_{123} u_1 u_2 u_3$$
$$+ \sum_{i\le j}\sum q_{iijj} u_i^2 u_j^2 + \sum_{i\neq j}\sum q_{iiij} u_i^3 u_j$$
$$+ \sum_i \sum_{j<k} \sum q_{iijk} u_i^2 u_j u_k + (\text{higher terms}).$$

Here $\mathbf{u}$ is the displacement vector, and u_1, u_2 and u_3 are the components along the x, y and z axes defined for the atom. Since the point symmetry of the Mn^{2+} and Ti^{4+} ions in the crystal of $MnTiO_3$ is 3, the potentials have the following form, if the anharmonic terms higher than fourth order are neglected,

$$\begin{aligned} V(\mathbf{u}) = V_0 &+ \tfrac{1}{2}[b_1(u_1^2+u_2^2)+b_3u_3^2] \\ &+ c_{111}(u_1^3-3u_1u_2^2)+c_{222}(u_2^3-3u_1^2u_2) \\ &+ c_{333}u_3^3+c_{311}(u_1^2u_3-u_2^2u_3) \\ &+ q_{1111}(u_1^4+u_1^2u_2^2+u_2^4)+q_{3333}u_3^4 \\ &+ q_{1133}(u_1^2u_3^2+u_2^2u_3^2)+q_{1131}(u_1^3u_3-3u_1u_2^2u_3) \\ &+ q_{2223}(u_2^3u_3-3u_1^2u_2u_3). \end{aligned}$$

The anharmonic parameters, c_{ijk}'s and q_{ijkl}'s, were refined together with the positional and harmonic parameters, b_1 and b_3, with the full-matrix least-squares program *LINKT80*, by fixing the population parameters. The R and R_w values reduced to 0·0118 and 0·0149, respectively.

Table 1. *Final positional, anisotropic thermal and anisotropic type* II *extinction parameters*

The form of the anisotropic temperature factor is defined as $\exp\{-2\pi^2[(h^2+k^2)a^{*2}U_{11}+l^2c^{*2}U_{33}+\frac{1}{2}hka^{*2}U_{11}]\}$.

Positional and thermal (Å^2) parameters

Mn	z	0·36002 (1)	O	x	0·3189 (1)
	U_{11}	0·00614 (4)		y	0·0310 (1)
	U_{33}	0·00655 (4)		z	0·24393 (3)
Ti	z	0·14758 (1)		U_{11}	0·0050 (1)
	U_{11}	0·00434 (3)		U_{22}	0·0062 (1)
	U_{33}	0·00472 (4)		U_{33}	0·0066 (1)
				U_{12}	0·00248 (9)
				U_{13}	0·00032 (8)
				U_{23}	0·00150 (8)

Extinction parameters (10^{-4} cm)

G_{11}	3·4 (1)	G_{12}	−2·0 (1)
G_{22}	1·2 (1)	G_{13}	0·5 (1)
G_{33}	4·1 (2)	G_{23}	−0·5 (1)

Table 2. *Harmonic* (10^{-19}J Å^{-2}), *third anharmonic* (10^{-19}J Å^{-3}) *and fourth anharmonic* (10^{-19}J Å^{-4}) *potential parameters at* 297 K, *with e.s.d.'s in parentheses*

	Mn	Ti
b_1	6·68 (0·06)	9·4 (0·1)
b_3	6·26 (0·04)	8·7 (0·07)
c_{111}	−0·27 (0·23)	0·05 (0·6)
c_{222}	−0·13 (0·22)	−0·6 (0·6)
c_{311}	1·0 (0·5)	−2·0 (1·5)
c_{333}	−0·27 (0·36)	−0·5 (1·0)
q_{1111}	−2·6 (1·3)	−2·1 (4·4)
q_{1133}	14·7 (9·1)	1·4 (31·5)
q_{3333}	−5·3 (3·0)	−6·0 (28·1)
q_{1131}	−5·4 (7·7)	20·2 (26·7)
q_{2223}	1·1 (7·4)	−2·1 (10·0)

The final positional and anisotropic thermal parameters are listed in Table 1 together with the extinction parameters, and the potential parameters in Table 2.*

Results and discussion

Fig. 1 shows the interatomic distances in the MnO_6 and TiO_6 octahedra. In accordance with the ionic radius of Mn^{2+} being larger than that of Ti^{4+}, the MnO_6 octahedron has a larger mean metal–O distance (2·195 Å) than the TiO_6 octahedron (1·980 Å). The O–O^{ii} distance on the shared face is the shortest of the O–O distances of the MnO_6 octahedron, whereas the shared edge O–O^{vi} is the shortest in the TiO_6 octahedron, as in $CoTiO_3$ (Kidoh *et al.*, 1984). The metal ions are shifted from the centres of the coordination octahedra towards the vacant octahedral sites

* A list of structure factors has been deposited with the British Library Lending Division as Supplementary Publication No. SUP 39186 (16 pp.). Copies may be obtained through The Executive Secretary, International Union of Crystallography, 5 Abbey Square, Chester CH1 2HU, England.

as in other ilmenite-type and corundum-type crystals. The ratio of the distance between the central cation and the O^{2-} ion on the shared face to that between the cation and the O^{2-} ion on the opposite face is quite large (1·109) in the smaller TiO_6 octahedron compared to the value (1·080) of the larger MnO_6 octahedron. However, the ratio of the distance between the cation and the shared face to that between the cation and the opposite face is much larger in the MnO_6 octahedron (1·848) than in TiO_6 (1·650). In fact, the former is the largest of the values in the ilmenite-type crystals analysed to date.

In the deformation density map (Fig. 2) obtained after the usual refinement, the highest peak is observed at a distance of 0·29 Å from the Mn^{2+} site on the threefold axis with a height of 0·71 e $Å^{-3}$. After the refinement with anharmonic thermal parameters, the height of this peak reduced significantly to 0·25 e $Å^{-3}$ (Fig. 3). The negative peaks around the Mn^{2+} site also markedly reduced the depths. Correspondingly, c_{311}, c_{111}, q_{1111}, q_{1133} and q_{3333} have larger absolute values than the respective standard deviations for Mn^{2+}. Therefore, a large part of the residual densities around the Mn^{2+} ion in Fig. 2 is presumed to be due to the anharmonicity of the thermal vibration of Mn^{2+}, though the R_w value reduced only slightly. On the other hand, as regards Ti^{4+} only c_{311} had a larger absolute value than its standard deviation among the anharmonic potential parameters, and the residual densities around the Ti^{4+} ion in Fig. 2 were not so markedly changed in the residual density map after the final refinement (Fig. 3). The only significant change is observed in the depth of the negative peak at the Ti^{4+} site. This reduced from −0·68 to −0·37 e $Å^{-3}$. Consequently, anharmonicity in the thermal vibration of the Ti^{4+} ion is almost negligible at room temperature compared with the experimental errors.

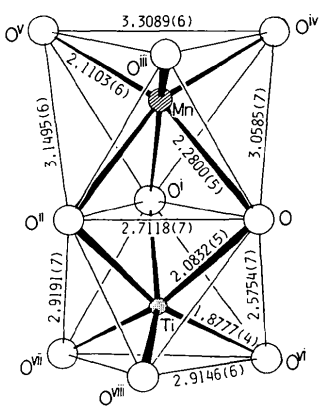

Fig. 1. Bond lengths (Å) in the MnO_6 and TiO_6 octahedra. Symmetry code: none x, y, z; (i) $-y, x-y, z$; (ii) $y-x, -x, z$; (iii) $\frac{1}{3}-x, \frac{2}{3}-y, \frac{2}{3}-z$; (iv) $\frac{1}{3}+y, \frac{2}{3}-x+y, \frac{2}{3}-z$; (v) $\frac{1}{3}+x-y, \frac{2}{3}+x, \frac{2}{3}-z$; (vi) $\frac{2}{3}-x, \frac{1}{3}-y, \frac{1}{3}-z$; (vii) $\frac{2}{3}+y, \frac{1}{3}-x+y, \frac{1}{3}-z$; (viii) $\frac{2}{3}+x-y, \frac{1}{3}+x, \frac{1}{3}-z$.

The minimum point of the negative peak at the Ti^{4+} site is not exactly at the cation site, but 0·03 Å from it. As seen in Fig. 3 the residual density around the Ti^{4+} ion has the same feature as that around the Ti^{4+} ion in $CoTiO_3$ (Kidoh *et al.*, 1984); namely, the electron cloud seems to be deformed to shield the positive charge of the neighbouring Mn^{2+} ion.

It is of interest to examine the difference Fourier map on the section through two neighbouring Mn^{2+} ions and two O^{2-} ions on the shared edge, since antiferromagnetic order was reported to remain in the (0001) plane even above the Néel temperature (Akimitsu *et al.*, 1970). This section of the difference Fourier map after the final refinement is shown in Fig. 4. There is a centre of symmetry at the centre of the square formed by four Mn–O bonds. The Mn–O–Mn angle is 88·41°. Interaction between the Mn^{2+} ions within the (0001) plane is believed to consist of

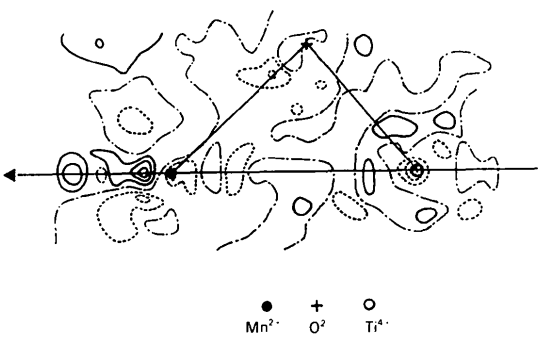

Fig. 2. Section of the difference Fourier map after the usual refinement, on the plane containing the Mn^{2+}, Ti^{4+} and O^{2-} ions. The filled and open circles indicate the Mn^{2+} and Ti^{4+} sites. The O^{2-} site is denoted with a cross. Contours are at intervals of 0·20 e $Å^{-3}$. Negative and zero contours are in broken and dashed-dotted lines, respectively.

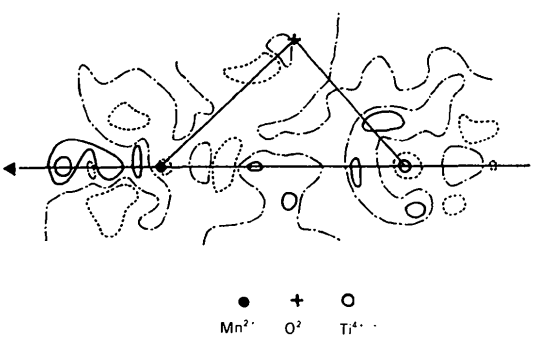

Fig. 3. Section of the difference Fourier map after the final refinement with anharmonic thermal parameters, on the plane containing the Mn^{2+}, Ti^{4+} and O^{2-} ions. The filled and open circles indicate the Mn^{2+} and Ti^{4+} sites. The O^{2-} site is denoted with a cross. Contours are at intervals of 0·20 e $Å^{-3}$. Negative and zero contours are in broken and dashed-dotted lines, respectively.

the contributions of direct Mn^{2+}–Mn^{2+} and 90° Mn^{2+}–O^{2-}–Mn^{2+} superexchange interactions (Goodenough & Stickler, 1967). The positive region spread between the Mn^{2+} ions suggests a significant contribution of the direct interaction, which is compatible with the antiferromagnetic order observed along the (0001) plane at low temperatures.

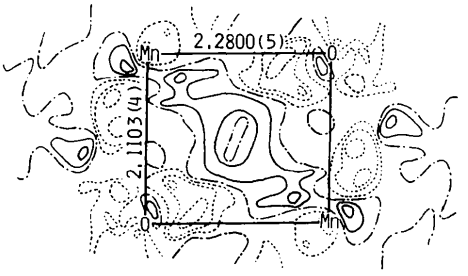

Fig. 4. Section of the difference Fourier map after the final refinement with anharmonic thermal parameters through the plane containing two neighbouring Mn^{2+} ions and the two O^{2-} ions on the shared edge. Contours are at intervals of 0·10 e Å^{-3}. Negative and zero contours are in broken and dashed-dotted lines, respectively. Distances are in Å.

Part of the research cost was met by a Grant-in-Aid for Scientific Research, No. 56420019, from The Ministry of Education, Science and Culture, to which the authors' thanks are due.

References

AKIMITSU, J., ISHIKAWA, Y. & ENDOH, Y. (1970). *Solid State Commun.* **8**, 87–90.
BECKER, P. J. & COPPENS, P. (1974*a*). *Acta Cryst.* A**30**, 129–147.
BECKER, P. J. & COPPENS, P. (1974*b*). *Acta Cryst.* A**30**, 148–153.
BECKER, P. J. & COPPENS, P. (1975). *Acta Cryst.* A**31**, 417–425.
BOND, W. L. (1951). *Rev. Sci. Instrum.* **22**, 344.
GOODENOUGH, J. B. & STICKLER, J. J. (1967). *Phys. Rev.* **164**, 768–778.
International Tables for X-ray Crystallography (1974). Vol. IV. Birmingham: Kynoch Press.
KIDOH, K., TANAKA, K., MARUMO, F. & TAKEI, H. (1984). *Acta Cryst.* B**40**, 92–96.
TAKEI, H., HOSOYA, S. & KOJIMA, H. (1982). *J. Jpn. Assoc. Mineral. Petrol. Econ. Geol.* Special Issue 3, pp. 73–82.
TANAKA, K. & MARUMO, F. (1984). To be published.
TOKONAMI, M. (1965). *Acta Cryst.* **19**, 486.
WILLIS, B. T. M. (1969). *Acta Cryst.* A**25**, 277–300.

Acta Cryst. (1984). B**40**, 332–337

Quantitative Analysis of CBED to Determine Polarity and Ionicity of ZnS-Type Crystals

BY K. ISHIZUKA*

Center for Solid State Science, Arizona State University, Tempe, AZ 85287, *USA*

AND J. TAFTØ†

Department of Physics, Arizona State University, Tempe, AZ 85287, *USA*

(*Received* 15 *October* 1983; *accepted* 23 *February* 1984)

Abstract

The possibility of determining the phase and amplitude of structure factors from convergent-beam electron-diffraction (CBED) patterns, where a few beams are simultaneously at the Bragg position, is studied by quantitative calculations. Dynamical calculations based on a new multislice formula for inclined illumination reproduce well the experimental CBED patterns of GaAs and verify the simple method for determining the absolute polarity of GaAs [Taftø & Spence (1982). *J. Appl. Cryst.* **15**, 60–64]. The calculations demonstrate the effect of the ionicity on the characteristic features of the $\bar{2}00$ disk. A qualitative comparison with experiments shows that the 200 structure factor of GaAs is close to, but slightly smaller than, that obtained from tabulated values for free atoms, suggesting a weak charge transfer from the Ga to the As atoms.

Introduction

Several electron diffraction techniques have been employed to determine structure-factor values. The Bragg reflections as well as the Kikuchi lines contain information about the absolute value of the structure factor and the phase relationship between the structure factors (Kambe, 1957), because many beams are simultaneously excited in most electron diffraction experiments. Two of the techniques, *i.e.* the critical-voltage method (Watanabe, Uyeda & Fukuhara, 1969) and the intersecting Kikuchi-line method (Gjønnes & Høier, 1971), have the advantages that they are essentially insensitive to crystal thickness. The former

* Present address: Institute for Chemical Research, Kyoto University, Uji 611, Japan.
† Present address: Metallurgy and Material Science Division, Brookhaven National Laboratory, Upton, New York 11973, USA.

0108-7681/84/040332-06$01.50